Genetic Evidence and Host Immune Response in Persons Reinfected with SARS-CoV-2, Brazil

Natalia Fintelman-Rodrigues, Aline P.D. da Silva, Monique Cristina dos Santos, Felipe B. Saraiva, Marcelo A. Ferreira, João Gesto, Danielle A.S. Rodrigues, André M. Vale, Isaclaudia G. de Azevedo, Vinícius C. Soares, Hui Jiang, Hongdong Tan, Diogo A. Tschoeke, Carolina Q. Sacramento, Fernando A. Bozza, Carlos M. Morel, Patrícia T. Bozza, Thiago Moreno L. Souza

The dynamics underlying severe acute respiratory syndrome coronavirus 2 (SARS-CoV-2) reinfection remain poorly understood. We identified a small cluster of patients in Brazil who experienced 2 episodes of coronavirus disease (COVID-19) in March and late May 2020. In the first episode, patients manifested an enhanced innate response compared with healthy persons, but neutralizing humoral immunity was not fully achieved. The second episode was associated with different SARS-CoV-2 strains, higher viral loads, and clinical symptoms. Our finding that persons with mild COVID-19 may have controlled SARS-CoV-2 replication without developing detectable humoral immunity suggests that reinfection is more frequent than supposed, but this hypothesis is not well documented.

Confirmed cases of severe acute respiratory syndrome coronavirus 2 (SARS-CoV-2) have surpassed 110 million, along with 2.5 million deaths by 2019 coronavirus disease (COVID-19) (*1*). New waves of the pandemics in different Northern and Southern Hemisphere countries provide evidence that herd immunity might not have been fully achieved and that new variants could escape the response to natural infection (*2*,*3*).

Although there is evidence of the generation of B and T memory cells to SARS-CoV-2 proteins after infection (*4*,*5*), it has also been documented that neutralizing seroconversion is heterogeneous among the population (*6*). Even for those who seroconvert, the sustainability of the immune response, as judged by IgG level, might decay after the primary exposure to coronaviruses (*7*–*9*). Cases of reinfection by SARS-CoV-2 can be associated with the absence of neutralizing serologic titers, diminishment of immunoglobulin titers after primo-infection, or viral polymorphisms to escape the host SARS-CoV-2 immune response (*10*–*16*).

To better understand the dynamics of the immune and virological responses in mild cases of COVID-19 that might predispose patients to reinfection, we continuously followed up with patients for potential exposure to SARS-CoV-2. For 2 patients, reinfection was documented. The National Review Board of Brazil approved the study protocol (Comissão Nacional de Ética em Pesquisa [CONEP] 30650420.4.1001.0008), and informed consent was obtained from all participants or patients' representatives.

Materials and Methods

Ethics and Study Population

During March–December 2020, the COVID-19 research task force screened a group of 30 participants weekly, independent of any symptoms, for SARS-CoV-2 detection by RT-PCR in nasopharyngeal swab specimens. If any of these participants exhibited positive results, or members of their households experienced signs or symptoms of COVID-19, they were invited to participate in the study and follow-up. At baseline and follow-up, we collected plasma, serum, and nasopharyngeal swab samples biweekly or at longer intervals if the patient was unavailable (Table). Households were included upon their request to be tested for SARS-CoV-2. Among

Author affiliations: Fundação Oswaldo Cruz (Fiocruz), Rio de Janeiro, Brazil (N. Fintelman-Rodrigues, A.P.D. da Silva, M.C. dos Santos, F.B. Saraiva, M.A. Ferreira, J. Gesto, I.G. de Azevedo, V.C. Soares, C.Q. Sacramento, F.A. Bozza, C.M. Morel, P.T. Bozza, T.M.L. Souza); Universidade Federal do Rio de Janeiro, Rio de Janeiro (D.A.S. Rodrigues, A.M. Vale, V.C. Soares, D.A. Tschoeke); MGI Tech Co., Ltd., Shenzhen, China (H. Jiang, H. Tan); D'Or Institute for Research and Education (F.A. Bozza)

DOI: https://doi.org/10.3201/eid2705.204912

the participants, 4 exhibited >1 episode of mild self-limiting COVID-19 with positive RT-PCR. For comparison, we included age-matched controls from the same group of participants and city in which the patients lived, Rio de Janeiro, Brazil. Controls were composed of 5 persons negative for SARS-CoV-2 throughout the investigated period.

Measurement of Serum SARS-CoV-2 Antibodies and Plasma Cytokine Levels

For quantitative analysis of SARS-CoV-2 spike protein IgM, IgA, and IgG antibodies, we performed the S-UFRJ test developed at Universidade Federal do Rio de Janeiro (R.G.F. Alvim et al., unpub. data, https://doi.org/10.1101/2020.07.13.20152884) (Appendix, https://wwwnc.cdc.gov/EID/article/27/5/20-4912-App1.pdf).

We collected plasma samples in tubes containing EDTA. We used commercial ELISA kits from R&D Systems (https://www.rndsystems.com) to measure cytokines and chemokine (Appendix).

Molecular Diagnosis

To determine serum titers to block SARS-CoV-2 infection, we performed miniaturized plaque-reduction neutralization test (PRNT) (Appendix). SARS-CoV-2 RNA has been detected in accordance with the US Centers for Disease Control and Prevention (CDC) recommendation (*17*). We used the standard curve method for virus quantification, using synthetic RNA for gene N (Microbiologics, https://www.microbiologics.com). We compared cycle thresholds (C_t) for the target gene to those obtained with different cell amounts (10^7–10^2), for reaction calibration (Appendix).

Genomic Analysis

We extracted total viral RNA from nasopharyngeal swabs using QIAamp Viral RNA (QIAGEN, https://www.qiagen.com), with minor modifications (*18*) (Appendix). We performed an amplicon-based enrichment strategy using the ATOPlex SARS-CoV-2 Full-Length Genome Panel version 1.0 (MGI Tech Co., https://en.mgi-tech.com; donated by the vendor). Single-stranded circular DNA library pools were converted to DNA nanoballs by rolling circle amplification and submitted to pair-end sequencing (100 nt) on the MGISEQ-2000 platform (recently named DNBSEQ-G400; MGI Tech Co. Ltd.).

We quality-scored, filtered, trimmed, and assembled genomic sequences in contigs through a validated workflow for SARS-CoV-2 (*19*). Genomes were aligned with MAFFT (*20*) or ClustalW (*21*), and phylogenies were constructed with MEGA version 7.0 (*22*,*23*), using the Jukes-Cantor model for maximum-likelihood estimates by applying neighbor-joining and BioNJ algorithms (*24*), or by MrBayes version 3.2.7 (http://nbisweden.github.io/MrBayes) (*25*,*26*) with a relaxed clock model with a priori model testing using the gamma rates and invariant sites nucleotide substitution model, selected by jModelTest version 1.6 http://darwin.uvigo.es/software/jmodeltest.htm. We visualized and edited the tree with FigTree version 1.4.2 (http://tree.bio.ed.ac.uk). We determined SARS-CoV-2 clades using the Nextclade software, beta version 0.14 (https://clades.nextstrain.org). To categorize mutations and polymorphisms, we aligned the SARS-CoV-2 reference genome Wuhan-Hu-1 (GISAID EPI ISL no. 402125; https://www.gisaid.org) to our sequences. The original sequences used in this work are publicly available on https://nextstrain.org/ncov: GISAID EPI ISL nos. 636737, 636834–636838. The dataset included in the analysis contained representative sequences of the emerging clades associated with our sequences, 19A and 20B, as well as sequences from the genome 20A as a negative control (Appendix Table 1).

Results

Among the households of the COVID-19 research task force, a 54-year-old man (patient A) requested an RT-PCR test for SARS-CoV-2 on March 23 because of a recurrent headache on the prior 2 days. He also had previous contact with a symptomatic co-worker returning from travel who refused to be tested. Patient A had a detectable viral load (C_t 27.41) of ≈10^5 copies/mL in nasopharyngeal swab samples (Table). Although patient B, a 57-year-old woman with a previous history of discoid lupus erythematosus, was in self-isolation, she was tested because of close contact with patient A. She tested positive for COVID-19 on March 24; her nasopharyngeal swab sample C_t was ≈36.31 (≈10^3 copies/mL) (Table). Two days afterward, she experienced diarrhea (Table).

Patient B shares a household with patients C and D, a married couple, both 34 years old. Patients C and D were not in social isolation because of their work duties. Although patient C was asymptomatic, he displayed a C_t of 35.71 (10^3 copies/mL) on March 25 (Table). Patient D was negative by molecular testing on March 26, but 1 week later, she had a detectable viral load (C_t 36.01, 10^3 copies/mL) and reported diarrhea in the following days (Table). On March 27, all 4 patients experienced an increase of inflammatory mediators (interleukin [IL] 6, IL-8, and tumor necrosis factor α) and regulatory (IL-10) and chemotactic (C-X-C motif chemokine ligand 10) and antiviral

(interferon γ) signals, relative to healthy SARS-CoV-2–negative controls (Figure 1). Although cytokine response was consistent with the resolution of the infection, the anti–SARS-CoV-2 neutralizing humoral response was not detected in late March 2020 (Table; Appendix Figure 2).

For patients B and C, we were able to obtain a full-length SARS-CoV-2 genome (Table). Complete genome sequencing, with Phred quality score >30, composed of 140,000–20,000,000 reads and 100-fold to 10,000-fold coverage, argues against a false-positive RT-PCR result (Appendix Table 2, first column). For patients A and D, the samples were insufficient for sequencing. In March 2020, patients B was infected with emerging SARS-CoV-2 clade 19A and patient C with SARS-CoV-2 clade 20B, (Table; Figure 2; Appendix Figure 3). The detection of the 2 distinct lineages indicates that patients B and C were infected independently and did not transmit the virus to each other (Table; Figure 2; Appendix Figure 3). These distinct lineages were co-circulating in Brazil in March 2020 when multiple introductions of the SARS-CoV-2 occurred (*27*). Emerging clade 19A is associated with imported cases in Brazil, because of its proximity to the Wuhan-01 sequence (Figure 2; Appendix Figure 3). Indeed, detection of clade 19A in the sample from Patient B is consistent with household transmission from patient A, and his contact with the symptomatic traveler. Patient C, a police officer, was frequently exposed to various probable sources of contamination; he was infected with an emerging clade 20B virus, the most prevalent variant in Brazil, during December 2020 (Figure 2; Appendix Figure 3). All patients recovered from a mild COVID-19 episode and were retested in the first half of April, when they had negative RT-PCR results.

In the last week of May 2020, when COVID-19 cases in Rio de Janeiro were at the peak of the first wave of the pandemic (*28*), these 4 patients reported more signs and symptoms of SARS-CoV-2 infection than in March (Table). During the second episode, they experienced fever and cough, along with fatigue, headache, body ache, anosmia, and ageusia. Real-time RT-PCR revealed higher viral loads in the nasopharyngeal swab samples than at the time of the first infection: C_t of 21.76 (≈10^7 copies/mL) for patient A, 21.84 (≈10^7 copies/mL) for patient B, 26.38 (≈10^5 copies/mL) for patient C, and 16.87 (≈10^9 copies/mL) for patient D (Table).

On June 3, a week after the second episode, we detected SARS-CoV-2 immunoglobulins in patients A and B, but they had low to no neutralizing activity (Table; Appendix Figure 2). These serologic samples from June indicate that the first episode of COVID-19 was not followed by a sustained neutralizing humoral response, as judged by 90% PRNT ($PRNT_{90}$) titers (Table). Because signals of a humoral effector memory were inconsistent after the first episode of COVID-19 (Table), we could speculate that the enhanced production of interferons and proinflammatory mediators led to resolution of the primo-infection (Figure 1). During the second episode of COVID-19, most of the cytokine levels were still higher than in healthy volunteers (Figure 1).

On July 9, forty days after the episode of reinfection, all patients had detectable immunoglobulin levels and their lowest $PRNT_{90}$ results (Table; Appendix Figure 2), declining thereafter by August 10 (Table; Appendix Figure 2). In July, patients' tests continuously showed upregulated pro-inflammatory markers (Figure 1), which are consistent with an enhanced

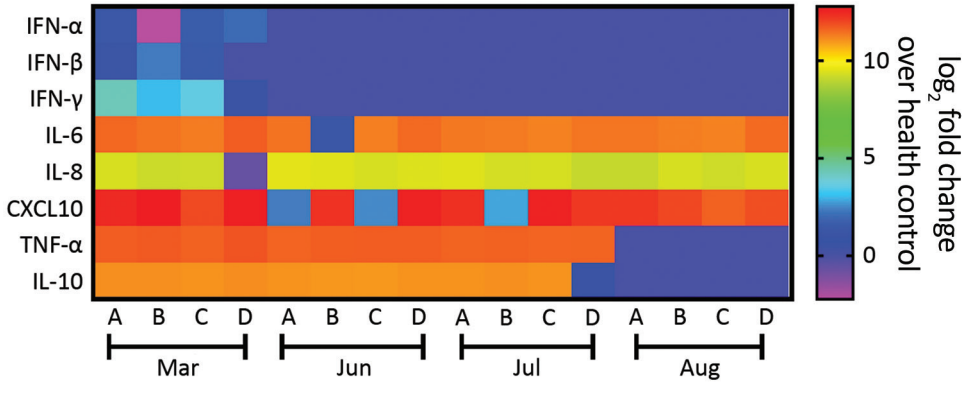

Figure 1. Heatmap showing the profile of innate immune response from patients who experienced 2 episodes of severe acute respiratory syndrome coronavirus 2 (SARS-CoV-2) infection, Brazil, 2020. We measured the mediators of innate immunity by ELISA for patients A–D. For comparison, these molecules were also quantified in the plasma from 5 healthy donors negative for SARS-CoV-2. The heatmap displays the $\log_2$ ratio of the fold-change from the plasma of the patients over the healthy volunteers. The means ± standard error of the means for the healthy volunteers were the following: IFN-α = 20.4 ± 4.7 pg/mL; IFN-β = 26.0 ± 3.9 pg/mL; IFN-γ = 27.8 ± 7.8 pg/mL; IL-6 = 13.4 ± 1.7 pg/mL; IL-8 = 137 ± 21.6 pg/mL; IL-10 = 165.4 ± 40.7 pg/mL; TNF-α = 33.8 ± 11.5 pg/mL; and CXCL-10 = 61.0 ± 27.3 pg/mL. CXCL, C-X-C motif chemokine ligand IFN, interferon; IL, interleukin; TNF, tumor necrosis factor.

Table. Characteristics of patients reinfected with severe acute respiratory syndrome coronavirus 2, Brazil, 2020*

Characteristic	Patient A	Patient B	Patient C	Patient D
Primo-infection				
Sex	M	F	M	F
Age, y	54	57	34	34
Concurrent conditions	None	Discoid lupus erythematosus	None	None
Date of symptom onset	March 21	March 26	Asymptomatic	March 31
Symptoms	Headache	Mild diarrhea	No	Mild diarrhea
N1 RT-PCR, log_{10} copies/mL	5.12	3.21	3.83	3.01
Date conducted	March 23	March 24	March 24	April 2
RNP RT-PCR (internal control), C_t	26.5	26.66	27.41	28.48
Serology†	IgM, IgA, IgG detected	IgM, IgA, IgG detected	IgM, IgA, IgG detected	IgM, IgA, IgG detected
$PRNT_{90}$/25 uL†	<1:4	<1:4	<1:4	<1:4
Sequencing	Not enough sample	Emerging clade 19A	Emerging clade 20B	Not enough sample
ID	N/A	EPI_ISL_636834	EPI_ISL_636836	NA
Second infection				
Date of onset illness	May 25	May 26	May 27	May 30
Symptoms	Fever, dry cough, tiredness, body ache, anosmia, ageusia	Fever, diarrhea, headache, body ache, anosmia, ageusia	Fever, nausea, tiredness, headache, body ache	Dry cough, diarrhea, tiredness, headache, body ache, anosmia, ageusia
RT-PCR, log_{10} copies/mL	7.31	7.42	5.18	9.61
Date conducted	May 29	May 29	May 29	May 29
RNP RT-PCR internal control	24.6	27.06	28.12	24.5
Serology results‡	IgM, IgA, IgG detected	IgM, IgA, IgG detected	IgM, IgA, IgG undetectable	IgM, IgA, IgG undetectable
$PRNT_{90}$/25 uL‡	1:16	<1:4	<1:4	<1:4
Sequencing	Emerging clade 20B	Emerging clade 20B	Emerging clade 20B	Emerging clade 20B
Accession ID	EPI_ISL_636737	EPI_ISL_636835	EPI_ISL_636837	EPI_ISL_636838
Follow-up				
Serology§	IgM, IgA, IgG detected	IgM, IgA, IgG detected	IgM, IgA, IgG detected	IgM, IgA, IgG detected
$PRNT_{90}$/25 uL§	1:128	1:32	1:64	1:64
Serology results¶	IgM, IgA, IgG detected	IgM, IgA, IgG detected	IgM, IgA, IgG detected	IgM, IgA, IgG detected
$PRNT_{90}$/25 uL	1:64	1:16	1:8	1:8

*N1, nucleocapside gene; NA, not available; $PRNT_{90}$, 90% plaque-reduction neutralization test; RNP, human RNase P gene; RT-PCR, reverse transcription PCR.
†Tests conducted March 27.
‡Tests conducted June 3.
§Tests conducted July 9.
¶Tests conducted August 10.

response to a second SARS-CoV-2 exposure. In August, the markers of inflammation and regulatory responses, tumor necrosis factor α and IL-10, decreased compared with levels from previous months (Figure 1).

In the second episode, we fully sequenced the SARS-CoV-2 genome from all patients (Table; Figure 2; Appendix Table 2, Figure 3). SARS-CoV-2 sequences from the reinfection clustered together, suggesting a household transmission for patients A–D (Figure 2; Appendix Figure 3). The emerging genotype 20B, which was the main variant circulating in Brazil since May 2020, was detected in all samples from the second episode (Figure 2; Table; Appendix Figure 3). For patient B, the first episode was associated with the emerging clade 19A and the second with 20B (Figure 2; Appendix Figure 3). Two episodes provoked by genetically distinct lineages support the possibility of reinfection.

Although both episodes in patient C were associated with clade 20B, they clustered apart on the phylogeny with significant statistical support: by 86% of bootstrap using maximum likelihood (Figure 2) and by Bayesian inference (Appendix Figure 3). Genetic markers in the SARS-CoV-2 genome were different in the patient's 2 episodes of COVID-19 (Appendix Table 2). The genomes diverge at the genes encoding the nonstructural protein (NSP) 3, 3C-like proteinase, and exonuclease (Appendix Table 2). In addition to the genetic variations, poor development of anti–SARS-CoV-2 serology between the 2 episodes of infection points suggests a reinfection scenario.

Discussion

Seasonal human coronaviruses may cause reinfection, as documented for the past 35 years (*8*,*29*). Of note, in veterinary medicine, domestic mammals also have coronavirus reinfection (*30*). Adaptive, memory-generating immunity to coronaviruses is heterogeneously sustainable in mammals, and some events of infection are controlled at the level of the

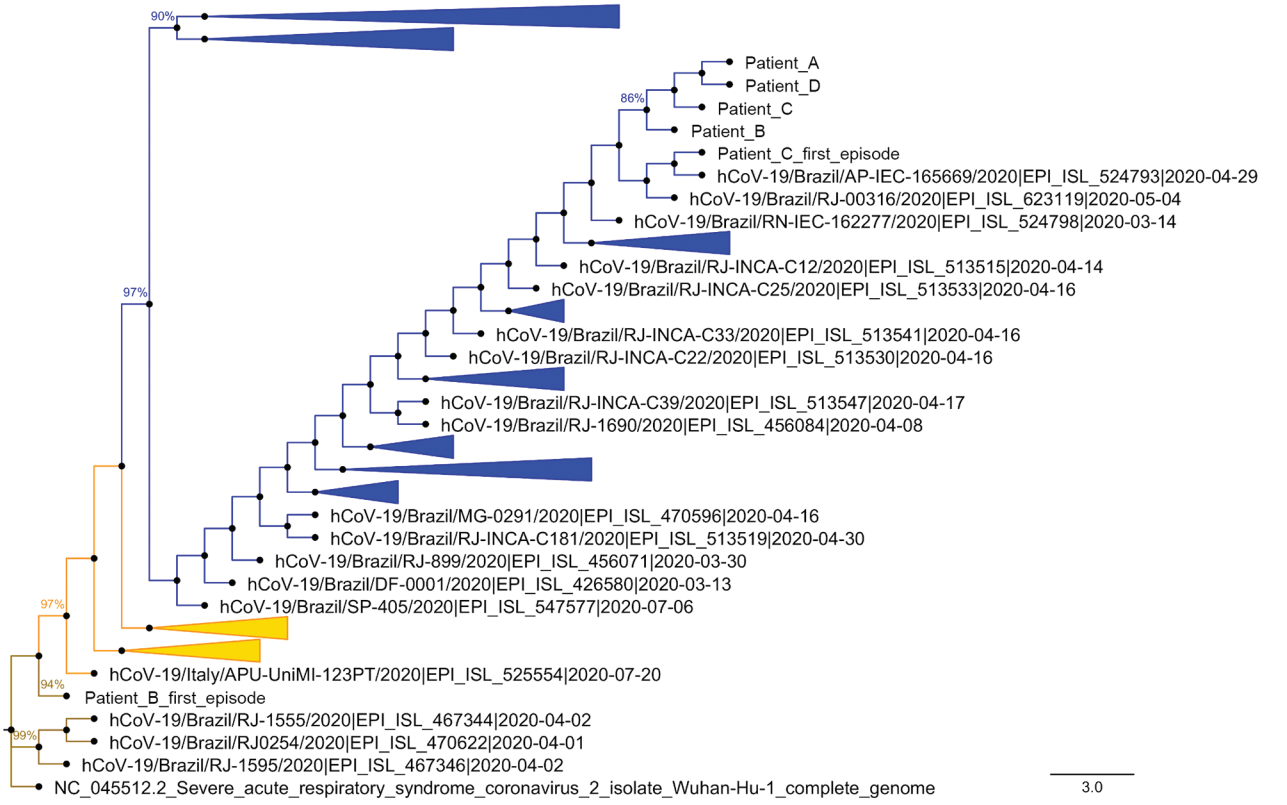

Figure 2. Phylogenetic analysis of severe acute respiratory syndrome coronavirus 2 genomes from reinfected patients, Brazil, 2020. Representative genomes deposited in GISAID (Appendix Table 1, Figure 3, https://wwwnc.cdc.gov/EID/article/27/5/20-4912-App1.pdf) were compared with sequences from virus genomes found in the respiratory samples from the first infection of patients B and C, and the second infection of patients A–D. A condensed phylogenetic tree rooted by reference genome Wuhan-Hu-1 (EPI_ISL_402125) was created with 1,000 bootstraps. Initial trees for the heuristic search were obtained automatically by applying neighbor-joining and BioNJ algorithms to a matrix of pairwise distances estimated using the Jukes-Cantor model (*24*), and then selecting the topology with a superior log-likelihood value. The tree with the highest log likelihood (−46487.36) is shown. The final dataset included a total of 29,920 positions. Evolutionary analyses were conducted in MEGA version 7.0 (*22*,*23*). Evolutionary history was inferred using the maximum-likelihood method and Jukes-Cantor model. Brown represents the emerging clade 19A, orange the clade 20A, and blue the clade 20B. Scale bar indicates substitutions per site. hCoV, human coronavirus.

innate immunity (*31*–*33*). We fully documented reinfection in 2 genetically unrelated persons in Rio de Janeiro, Brazil, describing patients who sought care twice in a 2-month interval who received clinical and laboratory diagnosis of COVID-19. Virus polymorphisms from the primary and second episodes and negative RT-PCR between the events strengthen the argument toward reinfection. Neutralizing anti–SARS-CoV-2 titers were not detected during the first episode, nor at the baseline of the second episode, suggesting that patients were still vulnerable after the primary episode.

SARS-CoV-2 reinfection has been associated with new variants that overcome the immune response to natural infection, short-lasting humoral response, and a limited or absent neutralizing immunity after the primo-infection (*10*–*13*). The patients in Brazil described in this study are similar to cases in the United States and Ecuador (*10*,*13*), in which reinfection was associated with more symptoms. Antibody-dependent enhancement or exposure to higher amounts of the virus could be the reason for the change from asymptomatic or oligosymptomatic to syndromic. In our study, primary and second infections were caused by a strain carrying the D614G mutation in the spike protein, which has been associated with higher replication efficiency (*34*). We did not detect other contemporaneous changes in the spike protein, such as 69/70 deletion, K417N, E484K, N501Y, P681H, or the 17 unique mutations of the P1 variant, which precluded association with more virulent strains (*35*). Beyond the spike protein, we detected the V125F change in the NSP14 protein; V125F is a nonconservative mutation that might increase the volume in the loop between β-sheets number 5 and 6, which could affect its methyltransferase activity (*36*).

The V125F mutation is unlikely to increase virulence in a second episode. On the other hand, changes in NSP6 protein (*37*) and open reading frame 6 mRNA (S. Sarif Hassan et al., unpub. data, https://doi.org/10.1101/2020.11.06.372227) might result in viral evasion from innate immunity.

The primary infections of patients B and C were associated with emerging clades 19A and 20B, indicating that the 2 cohabitants were infected independently. Indeed, while 1 patient was in social isolation, the others were working outside in the community. The cocirculation of these clades of SARS-CoV-2 is consistent with the COVID-19 databases in GISAID and the multiple introductions of the new coronavirus in Brazil (*27*). In the following months, emerging clade 20B was identified as the most prevalent genotype, representing 60% of the deposited genomes on GISAID. The detection of clade 20B on the second episode of COVID-19, by the end of May, is associated with the peak of the pandemic in Rio de Janeiro, Brazil (*28*).

Distinct clades of SARS-CoV-2 were found in the primary and secondary respiratory samples from patient B, supporting the notion of reinfection. For patient C, both the first and second detections of SARS-CoV-2 were associated with clade 20B. Although viral persistence could be imagined in this scenario, SARS-CoV-2 genomic sequences from the first and second episodes do not cluster together in the same branch, as they did for an immunocompromised patient that shed SARS-CoV-2 for 150 days (*38*). Thus, phylogeny does not support the interpretation of persistence, by different methods. By branching apart, SARS-CoV-2 genomes associated with patient C strengthen the chances of a relevant degree of variation (*39*), indicating the direction of reinfection. In the documented case of SARS-CoV-2 and human coronavirus NL63 reinfection, different episodes were genetically associated with similar viral clades or strains (*40*). Whereas the detection of 2 episodes of SARS-CoV-2 infection from patient C was separated by >60 days, prolonged virus shedding in the nasopharyngeal swab specimens from mild cases lasted for 22–46 days (*41*), which is further evidence against persistence.

Results of SARS-CoV-2 reinfection affirm that immune rechallenge may be necessary to achieve humoral protection and underscore that sustainability of the immune response may be heterogeneous. We documented that these patients with mild COVID-19 displayed an innate immune response composed of pro-inflammatory and regulatory signals. Although cytokine storm has been associated with severe COVID-19 (*42*), we interpret that in the case of our patients, the innate immune response might have led to infection resolution (*43*). Another possibility, not explored in detail here, is that cellular-mediated immunity could have contributed to the mild clinical outcome (*2*,*4*,*44*). The natural history of mild COVID-19 described for these patients might also be representative of many persons exposed to the first wave of the pandemic, leading to the hypothesis that they would also be susceptible to other episodes of SARS-CoV-2 infections, even without the challenge being imposed by new variants.

We determined, on the basis of 6 years of surveillance and follow-up of human coronavirus reinfections, that initial exposure was insufficient to elicit a protective immune response, imposing limited pressure on selection on new seasonal coronavirus variants (*40*). Similarly, our data on a small cluster of patients recapitulate this natural history of reinfection, which may also occur for SARS-CoV-2.

Acknowledgments

We thank Carmen Beatriz Wagner and Giacoia Gripp for assessments related to the Biosafety Level 3 facility and Marco Alberto Medeiros for assessments related to the sequencing platform. We thank Gonzalo Bello, Dumith Chequer Bou-Habib, Willian Provance, and Fabiano Thompson for insightful discussions. We greatly appreciated the MGI, a partner in the implementation of next-generation sequencing through collaborations with Oswaldo Cruz Foundation, especially for challenging samples of COVID-19.

Author contributions: F.A.B. and P.T.B. conducted clinical surveillance. N.F.R. and F.A.B. enrolled patients in the study. N.F.R., C.Q.S., D.R., I.G.A., V.C.S. performed immunologic assessments. N.F.R., A.P.D.S., M.C.S., F.B.S., M.A.F., J.G., H.J., and H.T. performed sequencing. A.P.D.S., M.C.S., and D.A.T were responsible for bioinformatics. F.A.B., P.T.B., C.M.M., T.M.L.S. handled study coordination. N.F.R., P.T.B., A.MV., and T.M.L.S. prepared and revised the manuscript. All authors revised and approved the manuscript.

About the Author

Dr. Fintelman-Rodrigues is based at the Laboratory of Immunopharmacology, Instituto Oswaldo Cruz (IOC), Fundação Oswaldo Cruz (Fiocruz), Rio de Janeiro, Brazil.

References

1. World Health Organization. Coronavirus disease (COVID-19) dashboard. 2020 [cited 2020 Nov 12]. https://covid19.who.int/
2. Rodda LB, Netland J, Shehata L, Pruner KB, Morawski PA, Thouvenel C, et al. Functional SARS-CoV-2-specific immune

memory persists after mild COVID-19. Cell. 2021;184:169–83. https://doi.org/10.1016/j.cell.2020.11.029 https://doi.org/10.1101/2020.08.11.20171843
3. Centers for Disease Control and Prevention. Cases, data, and surveillance. 2020 [cited 2021 Feb 12]. https://www.cdc.gov/coronavirus/2019-ncov/cases-updates/variant-surveillance/variant-info.html
4. Hartley GE, Edwards ESJ, Aui PM, Varese N, Stojanovic S, McMahon J, et al. Rapid generation of durable B cell memory to SARS-CoV-2 spike and nucleocapsid proteins in COVID-19 and convalescence. Sci Immunol. 2020;5:eabf8891. https://doi.org/10.1126/sciimmunol.abf8891
5. Le Bert N, Tan AT, Kunasegaran K, Tham CYL, Hafezi M, Chia A, et al. SARS-CoV-2-specific T cell immunity in cases of COVID-19 and SARS, and uninfected controls. Nature. 2020;584:457–62. https://doi.org/10.1038/s41586-020-2550-z
6. Ripperger TJ, Uhrlaub JL, Watanabe M, Wong R, Castaneda Y, Pizzato HA, et al. Detection, prevalence, and duration of humoral responses to SARS-CoV-2 under conditions of limited population exposure. Immunity. 2020;53:925–33. https://doi.org/10.1101/2020.08.14.20174490
7. Hueston L, Kok J, Guibone A, McDonald D, Hone G, Goodwin J, et al. The antibody response to SARS-CoV-2 infection. Open Forum Infect Dis. 2020;7:a387. https://doi.org/10.1093/ofid/ofaa387
8. Edridge AWD, Kaczorowska J, Hoste ACR, Bakker M, Klein M, Loens K, et al. Seasonal coronavirus protective immunity is short-lasting. Nat Med. 2020;26:1691–3. https://doi.org/10.1038/s41591-020-1083-1
9. Dan JM, Mateus J, Kato Y, Hastie KM, Yu ED, Faliti CE, et al. Immunological memory to SARS-CoV-2 assessed for up to 8 months after infection. Science. 2021;371:eabf4063. https://doi.org/10.1126/science.abf4063
10. Tillett RL, Sevinsky JR, Hartley PD, Kerwin H, Crawford N, Gorzalski A, et al. Genomic evidence for reinfection with SARS-CoV-2: a case study. Lancet Infect Dis. 2021;21:52–8. https://doi.org/10.1016/S1473-3099(20)30764-7
11. To KK-W, Hung IF-N, Ip JD, Chu AW-H, Chan W-M, Tam AR, et al. Coronavirus disease 2019 (COVID-19) reinfection by a phylogenetically distinct severe acute respiratory syndrome coronavirus 2 strain confirmed by whole genome sequencing. Clin Infect Dis. 2020 Aug 25 [Epub ahead of print]. https://doi.org/10.1093/cid/ciaa1275 https://doi.org/10.1093/cid/ciaa1275
12. Van Elslande J, Vermeersch P, Vandervoort K, Wawina-Bokalanga T, Vanmechelen B, Wollants E, et al. Symptomatic SARS-CoV-2 reinfection by a phylogenetically distinct strain. Clin Infect Dis. 2020 Sep 5 [Epub ahead of print].https://doi.org/10.1093/cid/ciaa1330 https://doi.org/10.1093/cid/ciaa1330
13. Prado-Vivar B, Becerra-Wong M, Guadalupe JJ, Marquez S, Gutierrez B, Rojas-Silva P, et al. COVID-19 reinfection by a phylogenetically distinct SARS-CoV-2 variant, first confirmed event in South America. SSRN. 2020 September 9 [cited 2021 Mar 19]. https://doi.org/10.2139/ssrn.3686174
14. Mulder M, van der Vegt DSJM, Oude Munnink BB, GeurtsvanKessel CH, van de Bovenkamp J, Sikkema RS, et al. Reinfection of severe acute respiratory syndrome coronavirus 2 in an immunocompromised patient: a case report. Clin Infect Dis. 2020 Oct 9 [Epub ahead of print]. https://doi.org/10.1093/cid/ciaa1538 https://doi.org/10.1093/cid/ciaa1538
15. Selhorst P, Van Ierssel S, Michiels J, Mariën J, Bartholomeeusen K, Dirinck E, et al. Symptomatic SARS-CoV-2 reinfection of a health care worker in a Belgian nosocomial outbreak despite primary neutralizing antibody response. Clin Infect Dis. 2020 Dec 14 [Epub ahead of print]. https://doi.org/10.1093/cid/ciaa1850 https://doi.org/10.1093/cid/ciaa1850
16. Larson D, Brodniak SL, Voegtly LJ, Cer RZ, Glang LA, Malagon FJ, et al. A case of early reinfection with severe acute respiratory syndrome coronavirus 2 (SARS-CoV-2). Clin Infect Dis. 2020 Sep 19 [Epub ahead of print]. https://doi.org/10.1093/cid/ciaa1436 https://doi.org/10.1093/cid/ciaa1436
17. Centers for Disease Control and Prevention. Research use only 2019-novel coronavirus (2019-nCoV) real-time RT-PCR primers and probes. 2020 [cited 2020 Nov 11]. https://www.cdc.gov/coronavirus/2019-ncov/lab/rt-pcr-panel-primer-probes.html
18. Metsky HC, Matranga CB, Wohl S, Schaffner SF, Freije CA, Winnicki SM, et al. Zika virus evolution and spread in the Americas. Nature. 2017;546:411–5. https://doi.org/10.1038/nature22402
19. Cleemput S, Dumon W, Fonseca V, Abdool Karim W, Giovanetti M, Alcantara LC, et al. Genome Detective coronavirus typing tool for rapid identification and characterization of novel coronavirus genomes. Bioinformatics. 2020;36:3552–5. https://doi.org/10.1093/bioinformatics/btaa145
20. Katoh K, Kuma K, Toh H, Miyata T. MAFFT version 5: improvement in accuracy of multiple sequence alignment. Nucleic Acids Res. 2005;33:511–8. https://doi.org/10.1093/nar/gki198
21. Larkin MA, Blackshields G, Brown NP, Chenna R, McGettigan PA, McWilliam H, et al. Clustal W and Clustal X version 2.0. Bioinformatics. 2007;23:2947–8. https://doi.org/10.1093/bioinformatics/btm404
22. Kumar S, Stecher G, Li M, Knyaz C, Tamura K. MEGA X: Molecular Evolutionary Genetics Analysis across computing platforms. Mol Biol Evol. 2018;35:1547–9. https://doi.org/10.1093/molbev/msy096
23. Felsenstein J. Confidence limits on phylogenies: an approach using the bootstrap. Evolution. 1985;39:783–91. https://doi.org/10.1111/j.1558-5646.1985.tb00420.x
24. Jukes TH, Cantor CR. Evolution of protein molecules. In: Mammalian protein metabolism. Vol. III. Munro HN, editor. New York: Academic Press; 1969. p. 21–132.
25. Huelsenbeck JP, Ronquist F. MRBAYES: Bayesian inference of phylogenetic trees. Bioinformatics. 2001;17:754–5. https://doi.org/10.1093/bioinformatics/17.8.754
26. Ronquist F, Huelsenbeck JP. MrBayes 3: Bayesian phylogenetic inference under mixed models. Bioinformatics. 2003;19:1572–4. https://doi.org/10.1093/bioinformatics/btg180
27. Candido DS, Claro IM, de Jesus JG, Souza WM, Moreira FRR, Dellicour S, et al.; Brazil-UK Centre for Arbovirus Discovery, Diagnosis, Genomics and Epidemiology (CADDE) Genomic Network. Evolution and epidemic spread of SARS-CoV-2 in Brazil. Science. 2020;369:1255–60. https://doi.org/10.1126/science.abd2161
28. Secretaria de Saúde do Estado do Rio de Janeiro. Covid-19 monitoring panel in the Rio de Janeiro State [in Portuguese]. 2020 [cited 2020 Nov 24]. http://painel.saude.rj.gov.br/monitoramento/covid19.html#
29. Kiyuka PK, Agoti CN, Munywoki PK, Njeru R, Bett A, Otieno JR, et al. Human coronavirus NL63 molecular epidemiology and evolutionary patterns in rural coastal Kenya. J Infect Dis. 2018;217:1728–39. https://academic.oup.com/jid/article/217/11/1728/4948258
30. Decaro N, Martella V, Saif LJ, Buonavoglia C. COVID-19 from veterinary medicine and one health perspectives: what animal coronaviruses have taught us. Res Vet Sci. 2020;131:21–3. https://doi.org/10.1016/j.rvsc.2020.04.009

31. Neeland MR, Bannister S, Clifford V, Dohle K, Mulholland K, Sutton P, et al. Innate cell profiles during the acute and convalescent phase of SARS-CoV-2 infection in children. Nat Commun. 2021;12:1084. https://doi.org/10.1038/s41467-021-21414-x
32. Tay MZ, Poh CM, Rénia L, MacAry PA, Ng LFP. The trinity of COVID-19: immunity, inflammation and intervention. Nat Rev Immunol. 2020;20:363–74. https://doi.org/10.1038/s41577-020-0311-8
33. Sallenave J-M, Guillot L. Innate immune signaling and proteolytic pathways in the resolution or exacerbation of SARS-CoV-2 in COVID-19: key therapeutic targets? Front Immunol. 2020;11:1229. https://doi.org/10.3389/fimmu.2020.01229
34. Groves DC, Rowland-Jones SL, Angyal A. The D614G mutations in the SARS-CoV-2 spike protein: Implications for viral infectivity, disease severity and vaccine design. Biochem Biophys Res Commun. 2021;538:104–7. https://doi.org/10.1016/j.bbrc.2020.10.109
35. Centers for Disease Control and Prevention. Emerging SARS-CoV-2 variants. 2020 [cited 2021 Feb 12]. https://www.cdc.gov/coronavirus/2019-ncov/more/science-and-research/scientific-brief-emerging-variants.html
36. Krafcikova P, Silhan J, Nencka R, Boura E. Structural analysis of the SARS-CoV-2 methyltransferase complex involved in RNA cap creation bound to sinefungin. Nat Commun. 2020;11:3717. https://doi.org/10.1038/s41467-020-17495-9
37. Cottam EM, Whelband MC, Wileman T. Coronavirus NSP6 restricts autophagosome expansion. Autophagy. 2014;10:1426–41. https://doi.org/10.4161/auto.29309
38. Choi B, Choudhary MC, Regan J, Sparks JA, Padera RF, Qiu X, et al. Persistence and evolution of SARS-CoV-2 in an immunocompromised host. N Engl J Med. 2020;383:2291–3.
39. Koyama T, Platt D, Parida L. Variant analysis of SARS-CoV-2 genomes. Bull World Health Organ. 2020;98:495–504. https://doi.org/10.2471/BLT.20.253591
40. Kiyuka PK, Agoti CN, Munywoki PK, Njeru R, Bett A, Otieno JR, et al. Human coronavirus NL63 molecular epidemiology and evolutionary patterns in rural coastal Kenya. J Infect Dis. 2018;217:1728–39. https://doi.org/10.1093/infdis/jiy098
41. Sun J, Xiao J, Sun R, Tang X, Liang C, Lin H, et al. Prolonged persistence of SARS-CoV-2 RNA in body fluids. Emerg Infect Dis. 2020;26:1834–8. https://doi.org/10.3201/eid2608.201097
42. de la Rica R, Borges M, Gonzalez-Freire M. COVID-19: in the eye of the cytokine storm. Front Immunol. 2020 ;11:558898. https://doi.org/10.3389/fimmu.2020.558898 https://doi.org/10.3389/fimmu.2020.558898
43. Arunachalam PS, Wimmers F, Mok CKP, Perera RAPM, Scott M, Hagan T, et al. Systems biological assessment of immunity to mild versus severe COVID-19 infection in humans. Science. 2020;369:1210–20. https://doi.org/10.1126/science.abc6261 https://doi.org/10.1126/science.abc6261
44. Sekine T, Perez-Potti A, Rivera-Ballesteros O, Strålin K, Gorin J-B, Olsson A, et al.; Karolinska COVID-19 Study Group. Robust T cell immunity in convalescent individuals with asymptomatic or mild COVID-19. Cell. 2020;183:158–168.e14. https://doi.org/10.1016/j.cell.2020.08.017

Address for correspondence: Thiago Moreno Lopes e Souza, Fundação Oswaldo Cruz (Fiocruz), Centro de Desenvolvimento Tecnológico em Saúde (CDTS), Instituto Oswaldo Cruz (IOC), Pavilhão Osório de Almeida, sala 16, Av. Brasil 4365, Manguinhos, Rio de Janeiro, RJ, CEP 21060340, Brazil; email: tmoreno@cdts.fiocruz.br

Article DOI: https://doi.org/10.3201/eid2705.204912

Genetic Evidence and Host Immune Response in Persons Reinfected with SARS-CoV-2, Brazil

Appendix

Detailed Materials and Methods

Measurement of Serum SARS-CoV-2 antibodies

For quantitative analysis of anti-SARS-CoV-2 spike protein IgM, IgA, and IgG antibodies, we performed the S-UFRJ test, as previously described (R.G.F. Alvim et al., unpub. data, https://doi.org/10.1101/2020.07.13.20152884). Briefly, high binding ELISA plates were coated with 50 μL of SARS-CoV-2 spike protein (4 μg/mL in phosphate-buffered saline [PBS]) and incubated overnight. The coating solution was removed, and 100 μL of PBS 1% BSA (blocking solution) was added, and the plate was incubated at room temperature (RT) for 1–2 h. The blocking solution was removed, and 50 μL of diluted 1:40 (PBS 1% BSA) patient serum specimens were added; subsequently, the specimens were serially 3-fold diluted in the plate, which was incubated at RT for 2 h. Then, the plate was washed with 150 μL of PBS (5×) and 50 μL of 1:10,000 goat anti-human IgG, IgA, and IgM (Fc)-horseradish peroxidase antibody (SouthernBiotech, https://www.southernbiotech.com) were added, and the plate was incubated for 1.5 h at RT. The plate was washed again with 150 μL of PBS (5×) and then treated with TMB (3,3‘, 5,5; -tetramethylbenzidine) (Scienco, http://www.scienco.bio.br) until the reaction was stopped with 50 μL of HCl 1N. The optical density (OD) was read at 450 nm with 655 nm background compensation in a microplate reader (Bio-Rad Laboratories, Inc., https://www.bio-rad.com).

Quantification of Plasma Cytokine Levels

Plasma samples from the acute and convalescent phases of the 2 episodes of SARS-CoV-2 infection were collected in EDTA-containing tubes. Tubes were placed on ice and aliquoted. Commercial ELISA kits (R&D Systems, https://www.rndsystems.com) were used to measure interferon (IFN)-α, -β and -γ, interleukin (IL)-6, −8 and −10, tumor necrosis factor α (TNF-α) and

induced protein 10 (IP10)/C-X-C motif chemokine ligand 10 (CXCL-10). This panel of mediators provides evidence for host production of antiviral, pro-inflammatory, and regulatory responses.

Plaque Reduction Neutralization Test (PRNT)

To determine serum titers to block SARS-CoV-2 infection, miniaturized PRNT was performed. In brief, human serum was heat-inactivated (30 min, 56°C) before 2-fold serial dilutions (from 1:4 to 1:2,056). Diluted serum specimens were incubated with 100 PFUs (PFU) of SARS-CoV-2 (GenBank accession no. MT710714) for 1 h at 37°C in 96-well plates. Afterward, mixtures of serum and virus were incubated with Vero E6 cells (2×10^4 cell/well) in 96-well plates for an additional 1 h at 37°C. Next, a fresh semisolid medium containing 2.4% of carboxymethylcellulose (CMC) was added to the wells, and cultures were maintained for 72 h at 37°C. Cells were fixed with 10% formalin for 2 h at room temperature and stained with crystal violet (0.4%). Endpoint dilution inhibiting 90% PFU ($PRNT_{90}$) was scored. As a control, to validate each assay, a back-titration of the mock-treated virus was included. Our quality control accepts the final readout of the virus input to be equivalent to 100 ± 20 PFU. Plaque numbers were scored in ≥ 3 independent experiments with technical replicates by 2 independent blinded readers to determine the $PRNT_{90}$ (Appendix Figure 1).

Molecular Diagnosis

The total viral RNA was extracted using QIAamp Viral RNA (QIAGEN, https://www.qiagen.com), according to the manufacturer's instructions. Quantitative RT-PCR was performed using GoTaq Probe qPCR and RT-qPCR Systems (Promega, https://www.promega.com) in a StepOne Real-Time PCR System (Thermo Fisher Scientific, https://www.thermofisher.com). Amplifications were carried out in 25 µL reaction mixtures containing 2× reaction mix buffer, 50 µM of each primer, 10 µM of the probe, and 5 µL of RNA template. Primers, probes, and cycling conditions used to detect the SARS-CoV-2 RNA were those recommended by the US Centers for Disease Control and Prevention (CDC) (*1*). The standard curve method was employed for virus quantification, using synthetic RNA for gene N (Microbiologics, Minnesota, USA). The C_t values for this target were compared with those obtained with different cell amounts (10^7 to 10^2), for reaction calibration.

Genomic Analysis

Total viral RNA from nasopharyngeal swabs was extracted using QIAamp Viral RNA (QIAGEN), with minor modifications (*2*). In brief, extraction was performed in 2 mL of sample/lysis buffer (1:1) without RNA carrier, and purified RNA was obtained after binding and

elution from a single silica column. For better yields, a 50-µL eluate was repetitively loaded (4×) to the same column. Tests were performed to evaluate if digestion with DNase I and depletion of rRNA enhanced the quantity/quality of SARS-CoV-2-related reads. Samples negative for SARS-CoV-2 and positive for Zika or chikungunya virus were included as controls.

To improve sequencing readout, an amplicon-based enrichment strategy was carried out with the ATOPlex SARS-CoV-2 Full-Length Genome Panel v1.0 (kindly donated by MGI Tech Co., https://en.mgi-tech.com). For library construction, RNA samples were first quantified with the Qubit RNA BR Assay Kit (Thermo Fisher Scientific), according to the manufacturer's instructions. Approximately 5 ng of each sample were then used as inputs to reverse transcription (RT) reactions, followed by two-step multiplex PCR-based genome amplification and dual adaptor indexing (i.e., barcoding) using proprietary primer sets. Products were purified with DNA Clean beads at a 5:6 volume ratio and subsequent washing steps with 80% ethanol. Next, individual libraries were quantified with the Qubit 1X dsDNA HS Assay Kit (Thermo Fisher Scientific) and homogeneously pooled to a total sum of 400 ng, before being submitted to denaturation, circularization, and digestion steps. Finally, single-stranded circular DNA library pools were converted to DNA nanoballs by rolling circle amplification and submitted to pair-end sequencing (100 nt) on the MGISEQ-2000 platform (recently named as DNBSEQ-G400; MGI Tech Co. Ltd).

Genomic sequences were quality-scored, filtered, trimmed, and assembled in contigs through a validated workflow for SARS-CoV-2 (*3*). Genomes were aligned with MAFFT (*4*) or ClustalW (*5*), and phylogenies were constructed with MEGA version 7.0 (*6,7*), using the Jukes-Cantor model for Maximum likelihood estimates, by applying neighbor-join and BioNJ algorithms (*8*). The tree with the highest log-likelihood was used. Alternatively, MrBayes version 3.2.7 (http://nbisweden.github.io/MrBayes) was used for Bayesian inference (*9,10*) with a relaxed clock model with a priori model testing using the gamma rates and invariant sites (G + I) nucleotide substitution model, selected by jModelTest version 1.6 http://darwin.uvigo.es/software/jmodeltest.htm (*11,12*). The tree was visualized and edited with FigTree version 1.4.2 (http://tree.bio.ed.ac.uk). SARS-CoV-2 clades were determined using the Web site https://clades.nextstrain.org. To categorize mutations and polymorphisms, the SARS-CoV-2 reference genome Wuhan-Hu-1 (GISAID EPI ISL no. 402125) was aligned to our sequences. The original sequences used in this work are publicly available on https://www.gisaid.org: GISAID EPI ISL nos. 636737, 636834–636838. The dataset included in the analysis contained representative sequences of the emerging clades associated with our

sequences, 19A and 20B, as well as sequences from the genome 20A as a negative control (Appendix Table 1).

References

1. Centers for Disease Control and Prevention. Research use only 2019-novel coronavirus (2019-nCoV) real-time RT-PCR primers and probes. 2020 [cited 2020 Nov 11]. https://www.cdc.gov/coronavirus/2019-ncov/lab/rt-pcr-panel-primer-probes.html

2. Metsky HC, Matranga CB, Wohl S, Schaffner SF, Freije CA, Winnicki SM, et al. Zika virus evolution and spread in the Americas. Nature. 2017;546:411–5. PubMed https://doi.org/10.1038/nature22402

3. Cleemput S, Dumon W, Fonseca V, Abdool Karim W, Giovanetti M, Alcantara LC, et al. Genome Detective coronavirus typing tool for rapid identification and characterization of novel coronavirus genomes. Bioinformatics. 2020;36:3552–5. PubMed https://doi.org/10.1093/bioinformatics/btaa145

4. Katoh K, Kuma K, Toh H, Miyata T. MAFFT version 5: improvement in accuracy of multiple sequence alignment. Nucleic Acids Res. 2005;33:511–8. PubMed https://doi.org/10.1093/nar/gki198

5. Larkin MA, Blackshields G, Brown NP, Chenna R, McGettigan PA, McWilliam H, et al. Clustal W and Clustal X version 2.0. Bioinformatics. 2007;23:2947–8. PubMed https://doi.org/10.1093/bioinformatics/btm404

6. Kumar S, Stecher G, Li M, Knyaz C, Tamura K. MEGA X: Molecular Evolutionary Genetics Analysis across computing platforms. Mol Biol Evol. 2018;35:1547–9. PubMed https://doi.org/10.1093/molbev/msy096

7. Felsenstein J. Confidence limits on phylogenies: an approach using the bootstrap. Evolution. 1985;39:783–91. PubMed https://doi.org/10.1111/j.1558-5646.1985.tb00420.x

8. Jukes TH, Cantor CR. Evolution of protein molecules. In: Mammalian protein metabolism. Vol. III. H. N. Munro, editor. New York: Academic Press; 1969. p. 21–132.

9. Huelsenbeck, J P, Ronquist F. MRBAYES: Bayesian inference of phylogeny. Bioinformatics. 2001;17:754–755

10. Ronquist, F, Huelsenbeck JP. MRBAYES 3: Bayesian phylogenetic inference under mixed models. Bioinformatics 2003;19:1572–1574.

11. Darriba D, Taboada GL, Doallo R, Posada D. jModelTest 2: more models, new heuristics and parallel computing. Nature Methods. 2012;9:772.

12. Guindon S, Gascuel O. A simple, fast and accurate method to estimate large phylogenies by maximum-likelihood. Systematic Biology. 2003;52:696–704

Appendix Table 1. Access codes for sequences used in tree construction compared with patients' virus sequences in study of patients reinfected with severe acute respiratory coronavirus 2, Brazil, 2020

No.	Name	Accession code
1	hCoV-19/Wuhan/Hu-1/2019	EPI_ISL_402125
2	hCoV-19/Brazil/RJ-UFRJ-9331/2020|EPI_ISL_492036|2020–06–01	EPI_ISL_492036
3	hCoV-19/Brazil/RJ-INCA-C44/2020|EPI_ISL_513551|2020–04–17	EPI_ISL_513551
4	hCoV-19/Brazil/RJ-INCA-C39/2020|EPI_ISL_513547|2020–04–17	EPI_ISL_513547
5	hCoV-19/Brazil/RJ-INCA-C38/2020|EPI_ISL_513546|2020–04–17	EPI_ISL_513546
6	hCoV-19/Brazil/RJ-INCA-C37/2020|EPI_ISL_513545|2020–04–16	EPI_ISL_513545
7	hCoV-19/Brazil/RJ-INCA-C36/2020|EPI_ISL_513544|2020–04–16	EPI_ISL_513544
8	hCoV-19/Brazil/RJ-INCA-C34/2020|EPI_ISL_513542|2020–04–16	EPI_ISL_513542
9	hCoV-19/Brazil/RJ-INCA-C33/2020|EPI_ISL_513541|2020–04–16	EPI_ISL_513541
10	hCoV-19/Brazil/RJ-INCA-C31/2020|EPI_ISL_513539|2020–04–16	EPI_ISL_513539
11	hCoV-19/Brazil/RJ-INCA-C30/2020|EPI_ISL_513538|2020–04–16	EPI_ISL_513538
12	hCoV-19/Brazil/RJ-INCA-C29/2020|EPI_ISL_513537|2020–04–16	EPI_ISL_513537
13	hCoV-19/Brazil/RJ-INCA-C27/2020|EPI_ISL_513535|2020–04–16	EPI_ISL_513535
14	hCoV-19/Brazil/RJ-INCA-C25/2020|EPI_ISL_513533|2020–04–16	EPI_ISL_513533
15	hCoV-19/Brazil/RJ-INCA-C24/2020|EPI_ISL_513532|2020–04–16	EPI_ISL_513532
16	hCoV-19/Brazil/RJ-INCA-C23/2020|EPI_ISL_513531|2020–04–16	EPI_ISL_513531
17	hCoV-19/Brazil/RJ-INCA-C22/2020|EPI_ISL_513530|2020–04–16	EPI_ISL_513530
18	hCoV-19/Brazil/RJ-INCA-C14/2020|EPI_ISL_513517|2020–04–14	EPI_ISL_513517
19	hCoV-19/Brazil/RJ-INCA-C13/2020|EPI_ISL_513516|2020–04–14	EPI_ISL_513516
20	hCoV-19/Brazil/RJ-INCA-C12/2020|EPI_ISL_513515|2020–04–14	EPI_ISL_513515
21	hCoV-19/Brazil/RJ-INCA-C07/2020|EPI_ISL_513514|2020–04–08	EPI_ISL_513514
22	hCoV-19/Brazil/RJ-INCA-C06/2020|EPI_ISL_513513|2020–04–08	EPI_ISL_513513
23	hCoV-19/Brazil/RJ-DCVN1/2020|EPI_ISL_509434|2020–03–23	EPI_ISL_509434
24	hCoV-19/Brazil/RJ-899/2020|EPI_ISL_456071|2020–03–30	EPI_ISL_456071
25	hCoV-19/Brazil/RJ-2072/2020|EPI_ISL_456104|2020–04–16	EPI_ISL_456104
26	hCoV-19/Brazil/RJ-1921/2020|EPI_ISL_456091|2020–04–09	EPI_ISL_456091
27	hCoV-19/Brazil/RJ-1719/2020|EPI_ISL_456088|2020–04–06	EPI_ISL_456088
28	hCoV-19/Brazil/RJ-1702/2020|EPI_ISL_456087|2020–04–08	EPI_ISL_456087
29	hCoV-19/Brazil/RJ-1690/2020|EPI_ISL_456084|2020–04–08	EPI_ISL_456084
30	hCoV-19/Brazil/RJ-1627/2020|EPI_ISL_456083|2020–04–03	EPI_ISL_456083
31	hCoV-19/Brazil/RJ-1595/2020|EPI_ISL_467346|2020–04–02	EPI_ISL_467346
32	hCoV-19/Brazil/RJ-1555/2020|EPI_ISL_467344|2020–04–02	EPI_ISL_467344
33	hCoV-19/Brazil/GO-L19-CD410/2020|EPI_ISL_476333|2020–04–02	EPI_ISL_476333
34	hCoV-19/Brazil/PR-5620/2020|EPI_ISL_541343|2020–03–20	EPI_ISL_541343
35	hCoV-19/Brazil/SP-193/2020|EPI_ISL_523984|2020–04–19	EPI_ISL_523984
36	hCoV-19/Brazil/SP-240/2020|EPI_ISL_524468|2020–05–01	EPI_ISL_524468
37	hCoV-19/Brazil/PE-IAM1126/2020|EPI_ISL_572379|2020–05–07	EPI_ISL_572379
38	hCoV-19/Brazil/SC-L15-CD265/2020|EPI_ISL_476259|2020–03–29	EPI_ISL_476259
39	hCoV-19/Brazil/SP-L14-CD257/2020|EPI_ISL_476253|2020–03–27	EPI_ISL_476253
40	hCoV-19/Brazil/SC-0244/2020|EPI_ISL_470653|2020–03–18	EPI_ISL_470653
41	hCoV-19/Brazil/AL-837/2020|EPI_ISL_427292|2020–03–18	EPI_ISL_427292
42	hCoV-19/Brazil/SP-294/2020|EPI_ISL_527862|2020–03–30	EPI_ISL_527862
43	hCoV-19/Brazil/SP-L5-CAMPI91/2020|EPI_ISL_476419|2020–04–23	EPI_ISL_476419
44	hCoV-19/Brazil/SP-254/2020|EPI_ISL_524469|2020–05–05	EPI_ISL_524469
45	hCoV-19/Brazil/SP-436/2020|EPI_ISL_603033|2020–07–13	EPI_ISL_603033
46	hCoV-19/Brazil/SP-441/2020|EPI_ISL_603038|2020–07–20	EPI_ISL_603038
47	hCoV-19/Brazil/RS-0242/2020|EPI_ISL_470651|2020–03–20	EPI_ISL_470651
48	hCoV-19/Brazil/SP-356/2020|EPI_ISL_547575|2020–06–16	EPI_ISL_547575
49	hCoV-19/Brazil/SP-321/2020|EPI_ISL_534316|2020–05–02	EPI_ISL_534316
50	hCoV-19/South_Korea/KCDC2712/2020|EPI_ISL_522491|2020–07–11	EPI_ISL_522491
51	hCoV-19/Brazil/PR-5621/2020|EPI_ISL_541344|2020–03–19	EPI_ISL_541344
52	hCoV-19/Brazil/SP-437/2020|EPI_ISL_603034|2020–07–11	EPI_ISL_603034
53	hCoV-19/Brazil/SP-433/2020|EPI_ISL_603030|2020–07–11	EPI_ISL_603030
54	hCoV-19/Brazil/UN-HIAE-SP04/2020|EPI_ISL_486429|2020–03–20	EPI_ISL_486429
55	hCoV-19/Norway/3069/2020|EPI_ISL_549084|2020–08–10	EPI_ISL_549084
56	hCoV-19/Brazil/SP-370/2020|EPI_ISL_583500|2020–06–29	EPI_ISL_583500
57	hCoV-19/Brazil/RJ-UFRJ-9331/2020|EPI_ISL_492036|2020–06–01	EPI_ISL_492036
58	hCoV-19/Thailand/Bangkok-0071/2020|EPI_ISL_445380|2020–03–30	EPI_ISL_445380
59	hCoV-19/Brazil/SP-439/2020|EPI_ISL_603036|2020–07–10	EPI_ISL_603036
60	hCoV-19/Brazil/SP-440/2020|EPI_ISL_603037|2020–07–20	EPI_ISL_603037
61	hCoV-19/Brazil/SP-394/2020|EPI_ISL_583503|2020–06–22	EPI_ISL_583503
62	hCoV-19/Brazil/SP-398/2020|EPI_ISL_603028|2020–06–30	EPI_ISL_603028
63	hCoV-19/Brazil/SP-L5-CAMPI77/2020|EPI_ISL_476416|2020–04–23	EPI_ISL_476416

No.	Name	Accession code
64	hCoV-19/Brazil/SP-283/2020|EPI_ISL_527860|2020–04–17	EPI_ISL_527860
65	hCoV-19/Ecuador/USFQ-004/2020|EPI_ISL_477014|2020–03–30	EPI_ISL_477014
66	hCoV-19/Ecuador/USFQ-020/2020|EPI_ISL_471267|2020–04–17	EPI_ISL_471267
67	hCoV-19/Ecuador/USFQ-039/2020|EPI_ISL_481245|2020–04–17	EPI_ISL_481245
68	hCoV-19/Ecuador/USFQ-1112/2020|EPI_ISL_486847|2020–06–30	EPI_ISL_486847
69	hCoV-19/Ecuador/USFQ-110/2020|EPI_ISL_486845|2020–06–30	EPI_ISL_486845
70	hCoV-19/Italy/APU-UniMI-123PT/2020|EPI_ISL_525554|2020–07–20	EPI_ISL_525554
71	hCoV-19/Brazil/GO-L19-CD413/2020|EPI_ISL_476336|2020–04–02	EPI_ISL_476336
72	hCoV-19/Brazil/MG-0288/2020|EPI_ISL_470593|2020–04–09	EPI_ISL_470593
73	hCoV-19/Brazil/RJ-0251/2020|EPI_ISL_470619|2020–03–27	EPI_ISL_470619
74	hCoV-19/Brazil/GO-0209/2020|EPI_ISL_470576|2020–04–03	EPI_ISL_470576
75	hCoV-19/Argentina/PAIS-A0023/2020|EPI_ISL_430814|2020–04–17	EPI_ISL_430814
76	hCoV-19/Luxembourg/LNS9470500/2020|EPI_ISL_434505|2020–04–08	EPI_ISL_434505
77	hCoV-19/Mexico/HID-InDRE-54/2020|EPI_ISL_576257|2020–07–22	EPI_ISL_576257
78	hCoV-19/Mexico/CMX-INMEGEN-02/2020|EPI_ISL_522873|2020–07–31	EPI_ISL_522873
79	hCoV-19/Peru/LIM-UPCH-0146/2020|EPI_ISL_568540|2020–08–28	EPI_ISL_568540
80	hCoV-19/Peru/LIM-INS-138/2020|EPI_ISL_536533|2020–03–17	EPI_ISL_536533
81	hCoV-19/Peru/LIM-INS-078/2020|EPI_ISL_536478|2020–07–02	EPI_ISL_536478
82	hCoV-19/Peru/LIM-UPCH-0160/2020|EPI_ISL_568553|2020–08–28	EPI_ISL_568553
83	hCoV-19/CotedIvoire/BKE0891/2020|EPI_ISL_614389|2020–08–18	EPI_ISL_614389
84	hCoV-19/Peru/LIM-INS-120/2020|EPI_ISL_536518|2020–05–05	EPI_ISL_536518
85	hCoV-19/Peru/LIM-UPCH-0138/2020|EPI_ISL_568534|2020–08–27	EPI_ISL_568534
86	hCoV-19/Turkey/KOC-IST-OD5/2020|EPI_ISL_613460|2020–06–21	EPI_ISL_613460
87	hCoV-19/USA/WI-UW-1054/2020|EPI_ISL_516480|2020–07–30	EPI_ISL_516480
88	hCoV-19/USA/WI-UW-759/2020|EPI_ISL_495464|2020–07–06	EPI_ISL_495464
89	hCoV-19/Peru/LIM-UPCH-0147/2020|EPI_ISL_568541|2020–08–28	EPI_ISL_568541
90	hCoV-19/USA/MI-MDHHS-SC22181/2020|EPI_ISL_614232|2020–10–12	EPI_ISL_614232
91	hCoV-19/USA/VA-DCLS-1506/2020|EPI_ISL_581508|2020–07–28	EPI_ISL_581508
92	hCoV-19/Peru/LIM-INS-100/2020|EPI_ISL_536499|2020–07–04	EPI_ISL_536499
93	hCoV-19/Mexico/CMX-INMEGEN-03/2020|EPI_ISL_522874|2020–07–31	EPI_ISL_522874
94	hCoV-19/Peru/LIM-UPCH-0127/2020|EPI_ISL_568523|2020–08–28	EPI_ISL_568523
95	hCoV-19/Peru/LIM-UPCH-0129/2020|EPI_ISL_568525|2020–08–28	EPI_ISL_568525
96	hCoV-19/Peru/LIM-UPCH-0128/2020|EPI_ISL_568524|2020–08–28	EPI_ISL_568524
97	hCoV-19/Romania/Mioveni-24095/2020|EPI_ISL_468156|2020–05–08	EPI_ISL_468156
98	hCoV-19/Mexico/TLA-InDRE-57/2020|EPI_ISL_576260|2020–08–13	EPI_ISL_576260
99	hCoV-19/Mexico/ZAC-InDRE-72/2020|EPI_ISL_576275|2020–08–14	EPI_ISL_576275
100	hCoV-19/France/BRE-BR9068/2020|EPI_ISL_613557|2020–09–06	EPI_ISL_613557
101	hCoV-19/Singapore/1110/2020|EPI_ISL_605819|2020–10–25	EPI_ISL_605819
102	hCoV-19/Netherlands/ZH-EMC-552/2020|EPI_ISL_577980|2020–09–08	EPI_ISL_577980
103	hCoV-19/Netherlands/ZH-EMC-607/2020|EPI_ISL_578035|2020–09–17	EPI_ISL_578035
104	hCoV-19/Brazil/SP-405/2020|EPI_ISL_547577|2020–07–06	EPI_ISL_547577
105	hCoV-19/Brazil/DF-0001/2020|EPI_ISL_426580|2020–03–13	EPI_ISL_426580
106	hCoV-19/Brazil/SP-345/2020|EPI_ISL_583495|2020–06–13	EPI_ISL_583495
107	hCoV-19/Brazil/PI-0239/2020|EPI_ISL_470613|2020–03–19	EPI_ISL_470613
108	hCoV-19/Brazil/RN-IEC-162277/2020|EPI_ISL_524798|2020–03–14	EPI_ISL_524798
109	hCoV-19/Brazil/RJ-INCA-C34/2020|EPI_ISL_513542|2020–04–16	EPI_ISL_513542
110	hCoV-19/Brazil/DF-891/2020|EPI_ISL_427298|2020–03–22	EPI_ISL_427298
111	hCoV-19/Brazil/DF-862/2020|EPI_ISL_427297|2020–03–23	EPI_ISL_427297
112	hCoV-19/Brazil/SP-399/2020|EPI_ISL_603029|2020–06–22	EPI_ISL_603029
113	hCoV-19/Ireland/D-NVRL-72IRL12139/2020|EPI_ISL_528465|2020–08–12	EPI_ISL_528465
114	hCoV-19/Brazil/MG-0291/2020|EPI_ISL_470596|2020–04–16	EPI_ISL_470596
115	hCoV-19/Brazil/RJ-00318/2020|EPI_ISL_623121|2020–05–12	EPI_ISL_623121
116	hCoV-19/Brazil/BA-L17-CD359/2020|EPI_ISL_476305|2020–03–31	EPI_ISL_476305
117	hCoV-19/Brazil/RJ-INCA-C181/2020|EPI_ISL_513519|2020–04–30	EPI_ISL_513519
118	hCoV-19/Brazil/AP-IEC-165669/2020|EPI_ISL_524793|2020–04–29	EPI_ISL_524793
119	hCoV-19/Brazil/RJ-0263/2020|EPI_ISL_470630|2020–04–13	EPI_ISL_470630
120	hCoV-19/Brazil/RJ-00364/2020|EPI_ISL_623167|2020–05–04	EPI_ISL_623167
121	hCoV-19/Brazil/RJ-UFRJ-58271/2020|EPI_ISL_492048|2020–06–01	EPI_ISL_492048
122	hCoV-19/Brazil/DF-615i/2020|EPI_ISL_427294|2020–03–13	EPI_ISL_427294
123	hCoV-19/Spain/GA-IBV-98006079/2020|EPI_ISL_541066|2020–07–03	EPI_ISL_541066
124	hCoV-19/Brazil/RJ-00316/2020|EPI_ISL_623119|2020–05–04	EPI_ISL_623119
125	hCoV-19/Argentina/PAIS-A0024/2020|EPI_ISL_430815|2020–04–18	EPI_ISL_430815
126	hCoV-19/Argentina/Heritas_HG001/2020|EPI_ISL_476496|2020–04–22	EPI_ISL_476496
127	hCoV-19/Argentina/Heritas_HG006/2020|EPI_ISL_476561|2020–05–07	EPI_ISL_476561
128	hCoV-19/Argentina/Heritas_HG007/2020|EPI_ISL_476565|2020–05–09	EPI_ISL_476565
129	hCoV-19/Argentina/Heritas-HG023/2020|EPI_ISL_615121|2020–05–26	EPI_ISL_615121
130	hCoV-19/Brazil/RJ-1466/2020|EPI_ISL_456081|2020–04–06	EPI_ISL_456081
131	hCoV-19/Brazil/RJ0272/2020|EPI_ISL_470638|2020–04–17	EPI_ISL_470638

No.	Name	Accession code
132	hCoV-19/Brazil/RJ0256/2020|EPI_ISL_470624|2020–04–03	EPI_ISL_470624
133	hCoV-19/Brazil/RJ0254/2020|EPI_ISL_470622|2020–04–01	EPI_ISL_470622
134	hCoV-19/Brazil/RJ0251/2020|EPI_ISL_470619|2020–03–27	EPI_ISL_470619
135	hCoV-19/Brazil/RJ0248/2020|EPI_ISL_470616|2020–03–24	EPI_ISL_470616
136	hCoV-19/Brazil/RJ-0720/2020	EPI_ISL_636836
137	hCoV-19/Brazil/RJ-01020/2020	EPI_ISL_636834
138	hCoV-19/Brazil/RJ-06020/2020	EPI_ISL_636737
139	hCoV-19/Brazil/RJ-01020–2/2020	EPI_ISL_636835
140	hCoV-19/Brazil/RJ-0720.2/2020	EPI_ISL_63683
141	hCoV-19/Brazil/RJ-0920/2020	EPI_ISL_63683

Appendix Table 2. Genetic characteristics of the SARS-CoV-2 sequences detected in patients who were infected twice, Brazil, 2020

	First episode of infection		Second episode of infection			
Characteristics of SARS-CoV-2 sequences	Patient B (% quasispecies)	Patient C (% quasispecies)	Patient A (% quasispecies)	Patient B (% quasispecies)	Patient C (% quasispecies)	Patient D (% quasispecies)
No. reads	>140K	>2.600K	>472K	>24.400K	>15.600K	>20.000K
Phred quality score	-Q35	-Q36	-Q33	-Q36	-Q36	-Q36
Depth of coverage, average ± SD	103.5 ± 1.24	2018.85 ± 31.53	350.85 ± 4.04	18426.125 ± 279.91	11753.53 ± 257.32	10061.58 ± 3701.20
Mutations						
NSP2 (AA)						
G1522A (none)	X					
NSP3 (AA)						
A6866G (N1383D)	X					
C3037T (none)	X	X (24.7)	X	X	X	X
C6021T (P1101L)	X (25.44)					
4151_4152delTT (L478X)		X				
C7164T (T1482I)		X (25.1)				
T7082A (S1455T)			X (25.3)			
A7384T (Q1555H)			X (25.3)			
NSP4 (AA)						
C9569T (P339S)			X (25.3)			
3C-like proteinase (AA)						
A10904G (S284G)		X (25.1)				
NSP6 (AA)						
C11514T (T181I)			X	X	X	X
RNA-dependent RNA polymerase (AA)						
G15406T (A656S)	X					
C14408T (P323L)	X (74.6)	X	X	X	X	X
A14836G (I466V)	X (24.77)					
Helicase (AA)						
A17105G (H290R)			X (25.3)			
3′-5′-Exonuclease						
G18412T (V125F)			X	X	X	X
G18180T (K47N)						X
18180_18181insTG (K47_D48insX)						X
EndoRNase						
A20265G (none)	X (25.44)					
2'-O-Ribose methyltransferase						
A21415T (K53*)	X (24.76)					
Surface glycoprotein						
A23403G (D614G)	X	X	X	X	X	X
T22619G (W353G)			X (25.3)			
Membrane glycoprotein						
G26795T (M91I)	X					
G27112A (S197N)	X (25.01)					
A26555N (E11X)	X (25.44)					
G26556N /A26557N/ G26558N (E12X)	X (25.44)					
C26559N (L13X)	X (25.44)					
27184_27228del TACAGTAAGTGACAA CAGATGTTTCATCTCGTTGACTTTCAGGTT (V221X)				X (24.7)		

	First episode of infection		Second episode of infection			
Characteristics of SARS-CoV-2 sequences	Patient B (% quasispecies)	Patient C (% quasispecies)	Patient A (% quasispecies)	Patient B (% quasispecies)	Patient C (% quasispecies)	Patient D (% quasispecies)
ORF6						
T27299C (133T)		X	X	X (75.3)	X	X
27184_27228delTACAGTAAGTGACAACAGATGTTTCATCTCGTTGACTTTCAGGTT (M1_V9del)				X (24.7)		
27196_27228delCAACAGATGTTTCATCTCGTTGACTTTCAGGTT (M1_V9del)					X (24.54)	
27197_27226delAACAGATGTTTCATCTCGTTGACTTTCAGG (M1_Q8del)					X (25.56)	
27197_27226delAACAGATGTTTCATCTCGTTGACTTTCAGG (V9X)					X (25.56)	
A27313G (K38E)						X
Nucleocapsid						
G28881A/G28882G (R203K)		X	X	X	X	X
G28883C (G204R)		X	X	X	X	X
T29148C (I292T)		X	X	X	X	X

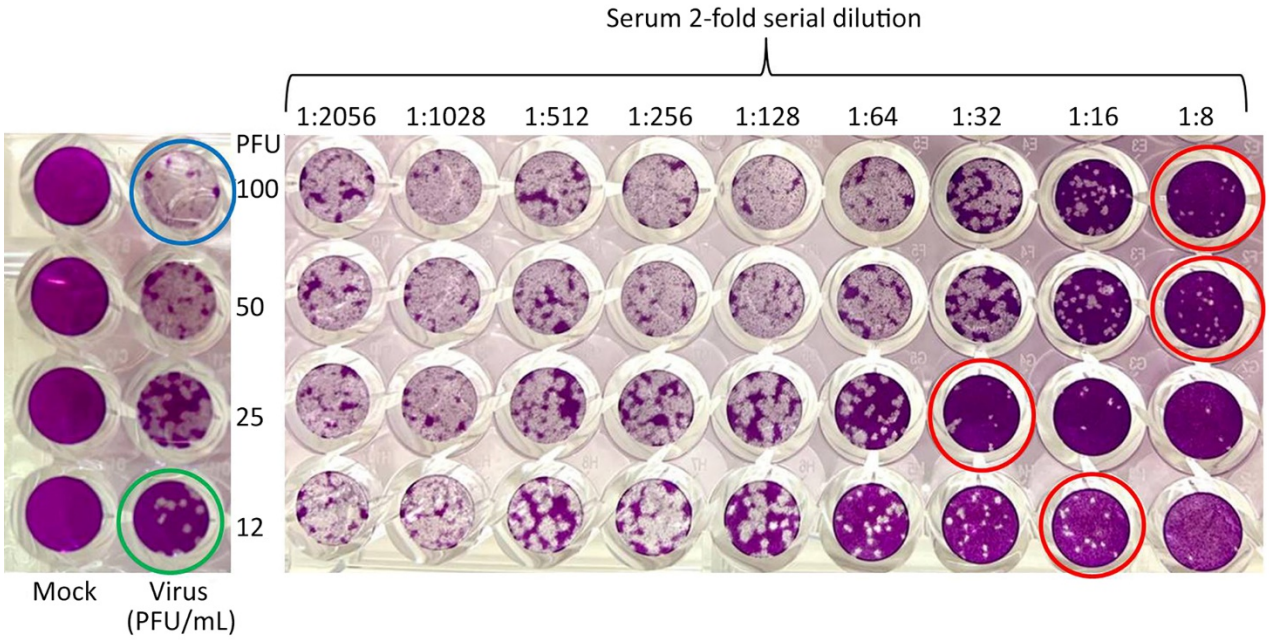

Appendix Figure 1. Representative readout of PRNT. 2-fold serial dilutions (from 1:4 to 1:2056) of human serum specimens were incubated in duplicates with ≈100 PFUs (PFU) of SARS-CoV-2. The serum–virus mixture was incubated for 1 h at 37°C and then added to Vero E6 cells (2×10^4 cell/well) in 96-well plates and incubated for an additional 1 h at 37°C. Next, a medium with 2.4% CMC was added. After 72 h at 37°C, cells are fixed with 10% formalin and stained with crystal violet (0.4%). Mock = uninfected control. To calculate virus PFU/mL, a back-titration of the mock-treated virus was included in each experiment, the undiluted virus input incubated with the serum is highlighted by the blue circle, a 2-fold serial dilution of the virus is shown, the last dilution of the virus input (1:8) produced 12/13 PFU (green circle), validating the assay. The endpoint dilution of the serum capable of neutralizing the virus input (blue circle) by 90% was expected to produce ≈10 PFU; these dilutions are shown by the red circles.

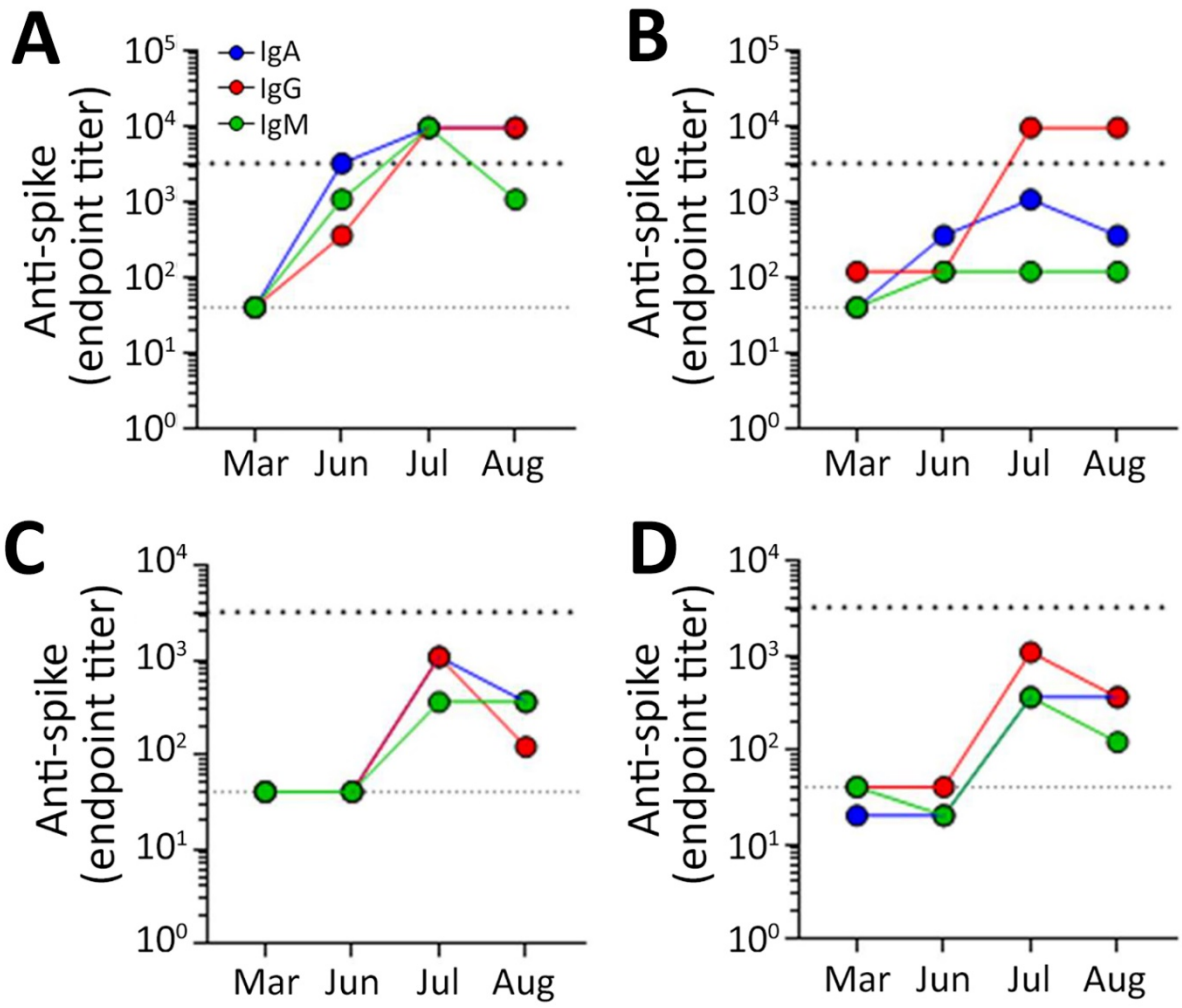

Appendix Figure 2. Quantitative analysis of IgA, IgM, and IgG from patients during the primary, second infections, and 2 months after the second infection. Plasma samples from patients were collected in March, June, July, and August for longitudinal detection of anti-Spike IgM (green), IgA (blue), and IgG (red) antibodies (A–D). The relative levels of antibodies were shown as endpoint titers of patient sample values for optical density [mean + 3 standard deviation (X + 3SD)] negative controls on the same ELISA plate. The dashed horizontal line represents the endpoint titer value between 10,000–30,000. The samples below the dotted line are considered negative.

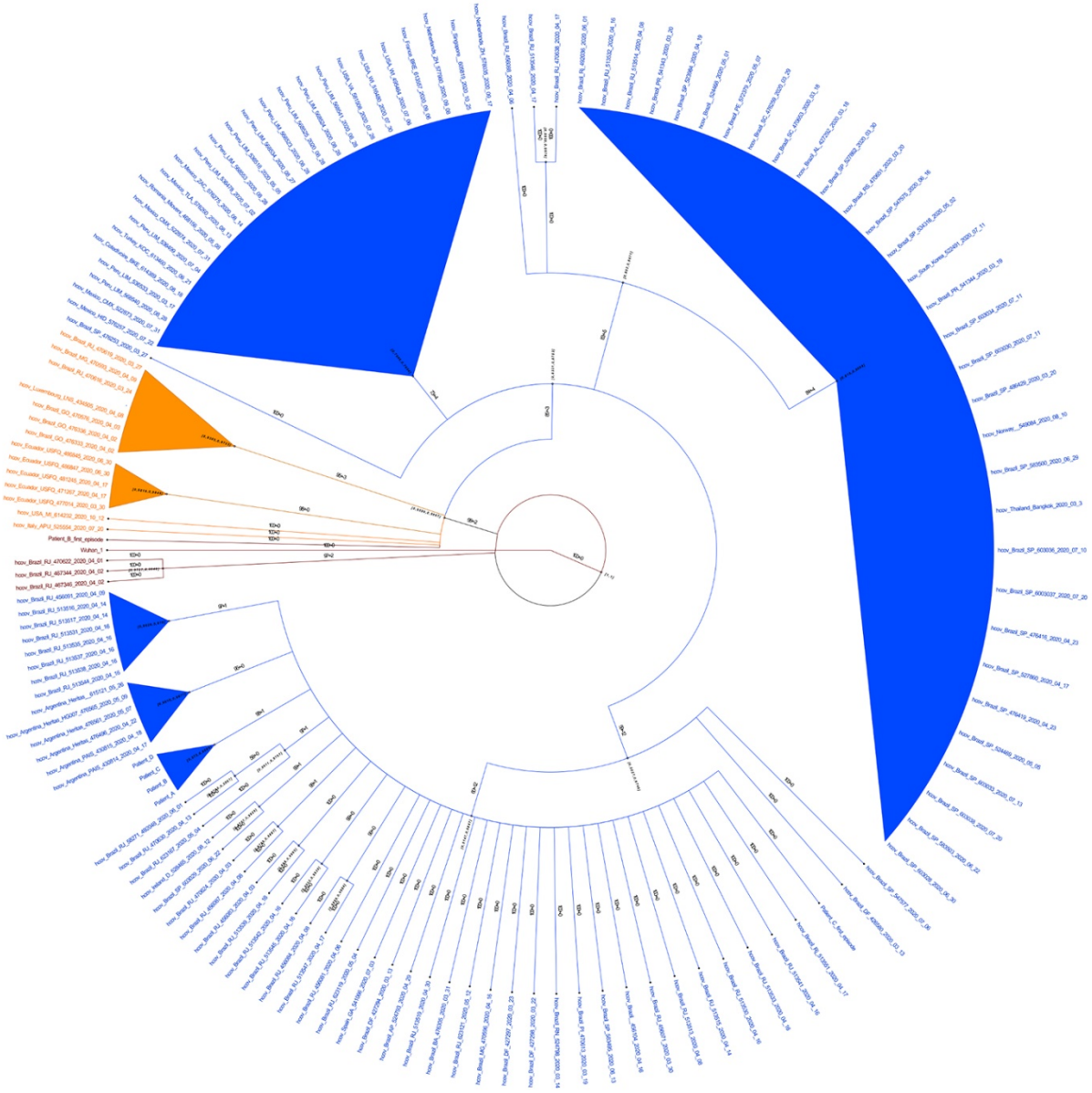

Appendix Figure 3. Phylogeny constructed by Bayesian inference using MrBayes version 3.2.7 (http://nbisweden.github.io/MrBayes), assuming a relaxed clock model with a priori model testing using the gamma rates and invariant sites nucleotide substitution model, selected by jModelTest version 1.6 (https://github.com/ddarriba/jmodeltest2). Emerging clade 19A is brown, clade 20A is orange, and clade 20B is blue. Posterior and anterior probabilities are presented for each branch.